Journal of
Synchrotron
Radiation

ISSN 0909-0495

Received 3 April 2008
Accepted 16 July 2008

Empirical dead-time corrections for synchrotron sources

D. A. Walko,* D. A. Arms and E. C. Landahl‡

Advanced Photon Source, Argonne National Laboratory, Argonne, IL 60439, USA.
E-mail: d-walko@anl.gov

An experimental comparison of models for performing dead-time corrections of photon-counting detectors at synchrotron sources is presented. The performance of several detectors in the three operating modes of the Advanced Photon Source is systematically compared, with particular emphasis on asymmetric fill patterns. Several simple and well known correction formulas are evaluated. The results demonstrate the critical importance of detector speed and synchrotron fill pattern in selecting the proper dead-time correction.

Keywords: dead-time; photon detector; synchrotron fill pattern; data correction.

1. Introduction

The dead-time of a photon-counting detector is the time needed for a detector to recover after counting a photon, before another photon can be counted. Dead-time corrections extend the usable range of a detector into a high-count-rate regime in which X-rays arrive too fast for all to be individually counted. Models for such corrections were originally based on Poisson statistics; that is, the intervals between X-rays arriving at the detector are assumed to be random and independent. In such cases, as a tube source, the dead-time constant τ is determined simply by how quickly the detector can recover after a counting event. At synchrotron X-ray sources, the time intervals between X-ray arrivals are not random but are determined by the fill pattern of electron bunches in the accelerator ring. For the most efficient use of a photon-counting detector, dead-time corrections which take into account the time structure of the X-ray source must be used. This article assesses various dead-time corrections for the main operating modes of the Advanced Photon Source (APS), comparing measurements made with two scintillator detectors and an avalanche photodiode (APD) detector. To our knowledge, this is the first systematic measurement of dead-time effects which studies variations in both the time structure of the source and the speed of the detector response. This is also, we believe, the first experimental investigation of dead-time effects in an asymmetric fill pattern. The results can be generalized to other synchrotron fill patterns and other detectors and could be used to optimize the data collection rate of an experiment.

The purpose of this paper is to determine the simplest and best dead-time correction for a given experimental condition, that is, for a given detector and the given source's pulse structure. We report tests on detectors with significantly different characteristics (speed and use of pulse-height analysis) in the various operating modes of the APS. §2 describes various dead-time models appropriate for synchrotron sources. In §3 and §4 we describe the fill patterns of the APS and our experimental set-up, respectively. In §5 we present the results and compare the accuracy of the various dead-time models.

2. Dead-time models

The model used in a dead-time correction will depend on the characteristics of the detector and the source. Several authors (*e.g.* Arndt, 1978; Quintana, 1991; Cousins, 1994; Kishimoto, 1997; Knoll, 2000; Bateman, 2000; Ida & Iwata, 2005) have developed a variety of dead-time models; in this section we will not derive them in detail but will review the models most appropriate for synchrotron sources. We will also present the effective dead-time τ for a given model, which may depend on the intrinsic detector speed, the extrinsic photon pulse rate, and whether pulse-height analysis (PHA) is used to discriminate between single-photon and multiphoton events. The ultimate goal is to be able to efficiently determine N_T, the true count rate, from N_O, the observed count rate, for a given experimental situation.

As a rule of thumb, at a source with bunch separation T, N_O is the product of three terms: the arrival frequency $1/T$, the probability of a countable event, and the fraction of time that the detector is rendered inoperative ('dead') owing to dead-time effects. By 'countable event' we mean a photon arriving at the detector which will be counted by the pulse-processing electronics, which depends on whether PHA is used. PHA is often implemented for scintillator detectors at synchrotrons to avoid contamination of the signal by higher harmonic photons; with PHA, a countable event is when one single photon arrives from a given bunch in the storage ring. (More advanced PHA techniques, which would determine the

‡ Current address: Department of Physics, DePaul University, Chicago, IL 60614, USA.

number of photons arriving from a given bunch, may lead to a complete solution for dead-time issues but will not be considered here.) The photons from a single bunch can be considered to have a Poisson distribution (Knoll, 2000). We use $P(j)$ to represent the probability of j photons arriving from one bunch, calculating it using Poisson statistics. The probability of arrival of one photon is

$$P(1) = N_{\rm T} T \exp(-N_{\rm T} T), \tag{1}$$

with the mean of the Poisson distribution being $N_{\rm T}T$. However, if PHA is not used, as is often the case with APDs, then a countable event occurs whenever one or more photons from a given bunch arrives at the detector. The probability of any number of photons arriving is the probability that zero photons do not arrive, that is,

$$\sum_{j=1}^{\infty} P(j) = 1 - P(0) = 1 - \exp(-N_{\rm T} T). \tag{2}$$

There are several ways to model the dead-time-induced inefficiency of a detector. In the non-extended dead-time model, the detector is considered inoperative for a fixed period of time τ after each observed photon; the dead-time-related efficiency of the detector is thus $(1 - \tau N_{\rm O})$. In the simplest and perhaps most common formulation of non-extended dead-time, the observed count rate is simply the product of the true count rate and the efficiency factor, which rearranges to give

$$N_{\rm T} = \frac{N_{\rm O}}{1 - \tau N_{\rm O}}. \tag{3}$$

Several authors (Arndt, 1978; Cousins, 1994; Kishimoto, 1997) have presented modifications of this formula to take into account the time structure of a synchrotron source.

However, most X-ray photon-counting detectors exhibit extended dead-time (Quintana, 1991; Bateman, 2000). In this case the detector is freshly rendered inoperative after each arriving photon. The detector recovery is delayed by the arrival of any photons during the detector's intrinsic recovery time $\tau_{\rm d}$. Together, $\tau_{\rm d}$ (which is due to the physical response of the photon-sensitive element plus the speed of the electronics) and T, the time separation of the synchrotron pulses, make up the two basic timescales of interest in dead-time corrections. We assume that the duration of a single X-ray bunch, of the order of 100 ps at the APS, is by far short enough to be neglected. According to the rule of thumb discussed above, the observed count rate for the extended dead-time model using PHA will be $(1/T)P(1)P(0)^{n-1}$. The integer n, which reflects the discrete nature of the source, is the number of bunches that occur in time $\tau_{\rm d}$. If a photon in a given bunch is to be counted, no photons must have arrived in the previous amount of time $\tau_{\rm d}$, that is, in the previous $n - 1$ bunches. The extended dead-time model, with PHA, then simplifies to

$$N_{\rm O} = N_{\rm T} \exp(-\tau N_{\rm T}), \tag{4}$$

where the effective dead-time is nT, or

$$\tau = T\big[{\rm Int}(\tau_{\rm d}/T) + 1\big]. \tag{5}$$

Here, the Int(x) function is the integer less than or equal to x. Equations (4) and (5) should generally be applicable to scintillators at synchrotron sources. The solution of (4) for $N_{\rm T}$ is called the Lambert W function (see Corless *et al.*, 1996); strategies for solution are discussed in Appendix *A*. Note that when the detector's intrinsic dead-time is less than the bunch separation, equation (5) simplifies to $\tau = T$ and the bunches are well separated. In the opposite limit, when $\tau_{\rm d} \gg T$, equation (5) yields $\tau \simeq \tau_{\rm d}$ as the source effectively appears continuous and the bunch structure becomes irrelevant.

Without PHA, single- and multiple-photon events are not distinguished and therefore the extended dead-time model gives an observed count rate of $(1/T)[1 - P(0)]P(0)^{n-1}$, or

$$N_{\rm O} = (1/T)\big[1 - \exp(-TN_{\rm T})\big]\exp\big[-(n-1)TN_{\rm T}\big]. \tag{6}$$

Although equation (6) does not have an analytic solution for $N_{\rm T}$, a recursive solution similar to that presented in Appendix *A* can be derived. An important limiting case of equation (6) occurs when the intrinsic detector response is significantly shorter than the separation of the synchrotron bunches ($\tau_{\rm d} < T$). This 'isolated' model, with $n = 1$, should represent APDs under most operating modes of a synchrotron, and simplifies to

$$N_{\rm T} = -(1/T)\ln\big(1 - N_{\rm O} T\big), \tag{7}$$

where the effective dead-time is simply the bunch period T. Equation (7) remains applicable for situations in which only photons from specific bunches are counted, such as an isolated bunch in a synchrotron's asymmetric fill pattern (see §2). Specific examples include the incident beam being mechanically chopped to periodically block some X-ray bunches, or the detector output being electronically gated to match the pump frequency in a pump–probe experiment. In these cases, T in (7) becomes the period of the bunch(es) of interest. Fig. 1 compares the non-extended, extended and isolated models described here. The observed count rates for the non-extended and isolated models eventually saturate at $1/\tau$ for high count rates, with the isolated model saturating quicker. The observed count rate for the extended model will reach a maximum and then decrease when $N_{\rm T} \geq 1/\tau$.

The dead-time correction of an asymmetric fill pattern is more difficult to model, since T varies between bunches. Lee & Mills (1992) derived a model in which they divided the fill pattern of charged particles in the accelerator into m groups, where a 'group' could be a collection of closely spaced

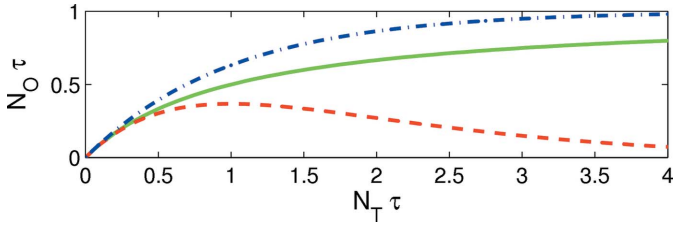

Figure 1
Comparison of observed and true count rates for the non-extended (solid line), extended (dashed line) and isolated (dash-dot line) dead-time models. The axes are normalized to the dead-time τ.

bunches, not necessarily individual bunches. In this model, bunches within a time τ_d can be grouped together, and are separated from other groups by at least τ_d. With α_i representing the fraction of charge in the ith group, and T_{period} representing the round-trip time of a bunch in the accelerator, then

$$N_O = N_T \sum_{i=1}^{m} \alpha_i \exp\left(-\alpha_i N_T T_{period}\right) \quad (8)$$

when PHA is used, and

$$N_O = 1/T_{period} \sum_{i=1}^{m} \left[1 - \exp\left(-\alpha_i N_T T_{period}\right)\right] \quad (9)$$

without PHA. In effect, different bunches in an asymmetric fill pattern will experience different dead-time effects. Again, this model requires τ_d to be longer than the group duration and shorter than the group separation. Monte Carlo simulations have been used to predict the dead-time behavior of asymmetric modes (Bateman, 2000), but to our knowledge these formulas have not been tested empirically.

3. Time structure of the APS ring

The APS accelerator is 1104 m in circumference, yielding a round-trip time of T_{period} = 3.682 μs; it normally operates with a current of 102 mA. The circulating electrons are grouped into bunches which can, in principle, fill the ring in a wide variety of patterns in any of its 1296 buckets. In practice, the APS in recent years has operated with three fill patterns. The standard operating mode, accounting for about 75% of operating time, fills the ring with 24 equally spaced bunches. The nominal current in this '24-bunch mode' is thus 4.2 mA per bunch, with a spacing of $T_{period}/24$ = 153 ns between bunches. In '324-bunch mode', every fourth bucket is filled with 0.31 mA per bunch for a separation of $T_{period}/324$ = 11.4 ns between bunches.

The final mode is an asymmetrically filled mode optimized for timing experiments. In this 'hybrid singlet mode', one singlet bunch is isolated from the others; this bunch is filled up to 16 mA. On the opposite side of the ring, eight sets of seven bunches ('septets') are filled equally with the remaining current, for 10.8 mA per septet. The singlet is separated from the nearest septets by a 1.59 μs gap on either side. The septets arrive at intervals of 68 ns, including the 17 ns width of each septet.

4. Experiment description

This series of experiments was performed at beamline 7ID of the APS. A double-crystal monochromator selected 10 keV X-rays from the undulator source. The second crystal of the monochromator was detuned to reduce spectral contamination from higher harmonics. In the 7ID-C experimental enclosure, motorized slits determined the incident X-ray flux, which was monitored by an ion chamber. The amplifier on the ion chamber was always set to keep its operation in the linear regime. Following the ion chamber, an amorphous material (Kapton or nylon) scattered X-rays into one of the photon-counting detectors used in this study, *i.e.* two scintillator detectors and one avalanche photodiode.

The two scintillator detectors are commonly used, commercially available detectors (Cyberstar). The first is a Tl-doped NaI scintillator crystal and an integrated electronics unit (model X1000, which includes an analog shaping amplifier, single-channel analyzer and high-voltage power supply). The peaking time of the amplifier on this detector, which we refer to as the 'NaI' detector, was 0.3 μs for all measurements reported here, which is well matched to the intrinsic decay time constant of NaI of about 230 ns. The second, referred to as the 'YAP' detector, is a Ce-doped $YAlO_3$ scintillator crystal with X2000 electronics. While YAP has poorer energy resolution and less efficiency at lower energies compared with NaI, its decay time constant is much shorter at 27 ns; a 50 ns peaking time was used for this detector. For both detectors, PHA was used by setting lower and upper discriminators in single-channel analyzers.

The APD detector used in this experiment was a model EG&G C30707 10 mm × 10 mm silicon APD built into a home-made amplifier circuit and aluminium housing that provided sufficient gain for single-photon counting with a constant fraction discriminator (CFD). Before the CFD, the amplifier produced a ∼10 ns duration electrical pulse; the CFD output duration was ∼30 ns.

In each measurement the count rates of the photon-counting detector and the monitoring ion chamber were recorded as the monochromatic X-ray flux was scanned from low to high. These measurements were performed for all detectors over the course of several months for each of the operating modes described above. The data collected in each operating mode were then fit to equations (3) and (4) for the scintillators, and equations (3) and (6) or (7), as appropriate, for the APD; the two fitting parameters were the effective dead-time τ and an overall scaling factor. This scale factor was first estimated in the low-count-rate regime, as the ratio of the count rates of the photon-counting detector and the ion chamber. The exact value of the scale factor depended on parameters such as the detector geometry, thickness of the amorphous material, and gain of the ion chamber's preamplifier; as such it varied from measurement to measurement. In the following section we present the true count rate N_T incident upon the scintillator detectors as the count rate of the ion chamber multiplied by the scale factor.

5. Results

Comparisons of the observed to the true count rates for both detectors in each mode are shown in Figs. 2, 3 and 4. Note the differences in scales on the three figures as the faster detectors progressively operate to higher count rates. The relatively slow NaI detector has almost the same behavior in the 324- and 24-bunch modes, since the dead-time correction is dominated by the detector response time. On the other hand, the YAP and APD detectors are sensitive to differences between these symmetric modes. Meanwhile, the dynamic range of all

detectors is relatively hampered in hybrid singlet mode. Also shown are best fits of the data to several models: the non-extended model [equation (3)] for all three detectors; the extended model with PHA [equation (4)] for the scintillators, and the extended model without PHA [equation (6)] or the isolated model [equation (7)] for the APD. Although both the YAP and APD detectors are fast enough to isolate bunches in 24-bunch mode, the use of PHA for the YAP but not the APD requires different models. Certainly, the non-extended dead-time model follows the general trend for all three detectors and could be used for a detector being operated somewhat beyond its linear response regime. However, the non-extended dead-time model tends to underestimate the correction in the middle of the range, typically by 2–5%, and overestimate it in the high-count-rate end of the range by 5% or more. The *R*-factor for fitting with the non-extended model was generally two to four times greater than for the more appropriate model.

Table 1
Comparison of measured and calculated dead-times in the applicable model.

Also shown are assumed values of τ_d for each detector. See text for details of the calculations.

Detector/τ_d (ns)	Operating mode	Effective τ (ns)		Model used
		Measured	Calculated	
NaI/600	324	731	602	Extended, with PHA
	24	749	614	Extended, with PHA
	Hybrid singlet	2186	2500	Lee & Mills, with PHA†
YAP/100	324	104	102	Extended, with PHA
	24	140	153	Extended, with PHA
	Hybrid singlet	493	415	Lee & Mills, with PHA†
APD/30	324	10.9	11.3	Extended, without PHA (n = 3)
	24	142	153	Isolated, without PHA
	Hybrid singlet	432	415	Lee & Mills, without PHA‡

† Data and model fit to equation (4). ‡ Data and model fit to equation (7).

The Lee & Mills (1992) calculations for the hybrid singlet case are also shown in the three figures. Differences in peaking times and use of PHA leads to three distinct dead-time models for this fill pattern. The NaI detector is too slow to resolve the septets, so there are two 'groups' of charge, with α_1 = 16/102 (the singlet) and α_2 = 86/102 (all the septets grouped together). Since the YAP and APD detectors can resolve the singlets, there are nine 'groups' of charge in this case; the singlet is still α_1 = 16/102, but the septets are α_i = 10.75/102 for i = 2 to 9. The detectors also vary in their PHA properties; equation (8) is appropriate for the NaI and YAP detectors with PHA, as is equation (9) for the APD without PHA.

In Table 1 we present the measured dead-times and compare them with the most appropriate model as described in §2. Uncertainties in the measured values of τ are typically 1–2%. In these calculations, τ_d is assumed to be the shaping time, *i.e.* twice the peaking time, for the scintillator detectors and the CFD output pulse duration for the APD. Comparing the measured and calculated values of τ for the scintillator detectors, it appears that the peaking time of 100 ns is an accurate value of τ_d for the YAP detector but 600 ns is an

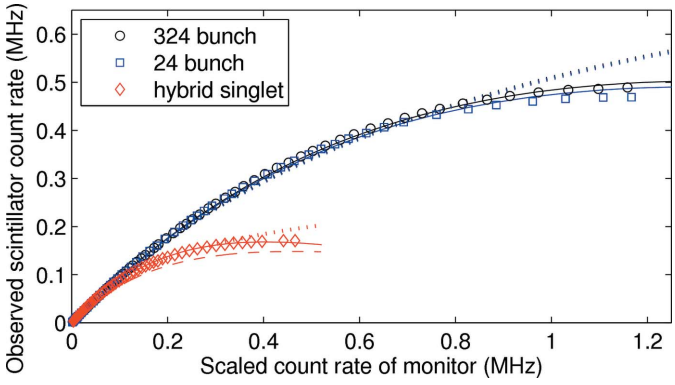

Figure 2
Response of the NaI detector in the three operating modes of the APS. The count rate of the ion chamber is scaled to that of the scintillator in the low-count-rate regime, and as such is treated as the 'true' count rate of the scintillator. For each operating mode, models of non-extended dead-time (dotted lines) and extended dead-time (solid lines) are shown. The dashed line for hybrid singlet mode is the model of Lee & Mills (1992), as explained in the text.

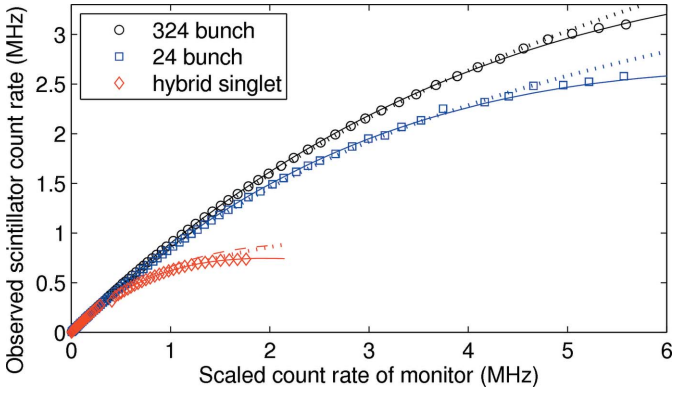

Figure 3
Response of the YAP detector in the three operating modes of the APS. Symbols are the same as in Fig. 2, but note the axes extend to count rates about five times higher.

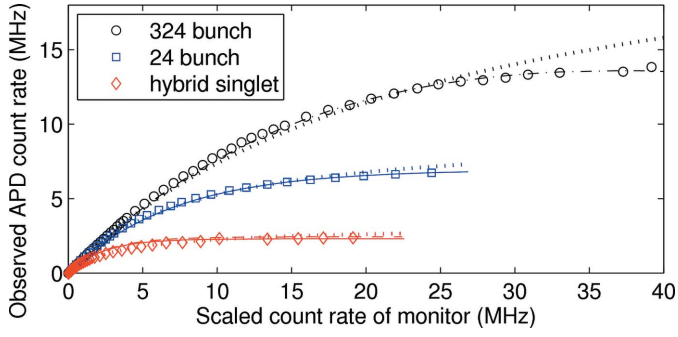

Figure 4
Response of the APD detector in the three operating modes of the APS. The dotted lines represent the non-extended dead-time model. The solid line corresponds to the isolated-bunch model in 24-bunch and hybrid singlet modes. The dash-dot line in 324-bunch mode is the extended dead-time model without PHA. The dashed line for hybrid singlet mode is the model of Lee & Mills (1992), which essentially overlaps the fit using the isolated-bunch model.

underestimate for the NaI detector. Using equation (5) to compare the measurements in 24- and 324-bunch modes, a more accurate value of τ_d for the NaI detector is 720 ns. The isolated model does not fit the APD data in 324-bunch mode as well as it does in 24-bunch mode. Since the output of the CFD is longer than the bunch separation in 324-bunch mode, the bunches are not truly isolated. Thus, equation (6) should be used rather than equation (7), with $n = 3$. Ideally one would use faster electronics with an APD in a mode with such closely spaced bunches. When the output of the APD is gated to an individual bunch in 24-bunch mode (not shown), the isolated-bunch model applies just as well as for the ungated APD; the best-fit time constant was 3.61 µs, which compares with T_{period} as expected.

The equations for hybrid singlet mode are not very convenient to use in practice, since neither equation (8) or equation (9) is analytically solvable for N_T. Therefore, we fit the results of these calculations as described above to equation (4) and equation (7), respectively, to obtain the calculated values of τ listed in Table 1. The experimental data in this mode also have good fits to equations (4) and (7), as seen in Figs. 2–4. However, there are differences of ~20% between the values of τ fit from the scintillator data and from the fits to the models, as listed in Table 1. The discrepancies are probably due to a breakdown in one of the assumptions of the model. For the YAP detector, whose calculated τ underestimates the measured value, the limiting assumption is probably that the septets can be completely separated into non-interacting groups; τ_d is, in fact, slightly longer than the septet separation. For the NaI detector, in which the calculation overestimates τ, the error may arise from the assumption that bunches arriving within a group can be treated as arriving simultaneously. In this case, the relevant 'group' is the whole train of septets, 500 ns long in all, whose duration is comparable with τ_d.

6. Conclusion

We have demonstrated the need for using the appropriate dead-time model with a proper value of the effective dead-time parameter in order to accurately correct high-count-rate data at a pulsed synchrotron source. The extended dead-time model with PHA was best for scintillator detectors, and the isolated-bunch model without PHA was usually appropriate for APDs. Specific models were, within their ranges of validity, fairly accurate at predicting the effective dead-time τ to use, but for best results τ should be measured whenever possible and its empirical value used.

The non-extended model is, perhaps, the more popular of dead-time corrections, with the advantage of a simple mathematical formula. Since all of the corrections discussed here are similar to first order, the non-extended model can be used for a detector operating slightly beyond its linear-response regime, but it is not generally trustworthy over a detector's full dynamic range. For example, if the non-extended model [equation (3)] is used to correct data from a detector that obeys the non-extended model, the resulting systematic error will be under 1% as long as the true count rate is $0.15/\tau$ or below.

These results can provide guidance in the development of future storage-ring operating modes. Certainly, detector dead-time is not the only factor to consider when designing a fill pattern, but it is one issue to address. For example, doubling the number of bunches in the standard mode of the APS from 24 to 48 would not improve the performance of the NaI or the YAP detector [as calculated by equation (5)], although it should cut the APD's dead-time by one half. Fewer bunches will worsen τ for all three detectors and would be an additional disadvantage to those experiments which benefit from a quasi-continuous source. These results can also be used in designing asymmetric fill patterns, which must balance the need of experiments requiring special timing patterns with the need of reasonable, predictable dead-times for other experiments.

APPENDIX *A*
Solutions of the extended dead-time model

The equation for the extended dead-time model with pulse-height analysis, equation (4), is called the Lambert W function (Corless *et al.*, 1996). Various approximations exist for finding N_T, the true count rate. One solution is found in a Taylor expansion (Corless *et al.*, 1996),

$$N_T = N_O \sum_{n=1}^{\infty} \frac{(n\tau N_O)^{n-1}}{n!}, \qquad (10)$$

which will converge over the range of N_O for which equation (4) is applicable, that is, for $N_T\tau < 1$. Alternatively, one can use the following recursive algorithm based on the Newton–Raphson method to solve $N_O = N_T \exp(-\tau N_T)$ for the true count rate N_T. In this algorithm, N_G is a guess for the true count rate at each step, N_R is the resulting value of the observed count rate, and ε is the required accuracy, which can easily be 1 count s^{-1}.

(i) Check observed rate. The maximum possible value for N_O is $(\tau e)^{-1}$, so the algorithm should stop with an error if $N_O > (\tau e)^{-1}$.

(ii) Initialize guess. Set $N_G \leftarrow N_O$. This is reasonable as an initial guess as N_O is never greater than N_T.

(iii) Calculate resultant rate. Compute $N_R \leftarrow N_G \exp(-\tau N_G)$.

(iv) Finished? If $(N_O - N_R) < \varepsilon$, the guess is sufficiently close; set $N_T \leftarrow N_G$ and exit the procedure.

(v) Improved guess. Use

$$N_G \leftarrow N_G + \left[\frac{\exp(\tau N_G)}{1 - \tau N_G}\right](N_O - N_R).$$

The guess is increased by the resulting discrepancy, scaled by the slope of the function. Go back to step (iii).

This recursion relation converges much faster than equation (10). N_T is approached from below, which ensures the algorithm does not arrive at the $N_T\tau > 1$ solution for a given N_O (see Fig. 1). As an example, for $\tau = 150$ ns and $\varepsilon = 1$ count s^{-1}, this recursion relation converges within nine iterations up to

the maximum true count rate of $1/\tau$, whereas equation (10) requires hundreds of terms for similar accuracy.

We thank John Quintana for helpful discussions, Steve Ross for supplying APDs, the APS Detector Pool for equipment loans, and the staff of beamline XOR/7ID for providing the beam time used for these measurements. Use of the APS was supported by the US Department of Energy, Office of Science, Office of Basic Energy Sciences, under Contract No. DE-AC02-06CH11357.

References

Arndt, U. W. (1978). *J. Phys. E*, **11**, 671–673.
Bateman, J. E. (2000). *J. Synchrotron Rad.* **7**, 307–312.
Corless, R. M., Gonnet, G. H., Hare, D. E. G., Jeffrey, D. J. & Knuth, D. E. (1996). *Adv. Comput. Math.* **5**, 329–359.
Cousins, C. S. G. (1994). *J. Appl. Cryst.* **27**, 159–163.
Ida, T. & Iwata, Y. (2005). *J. Appl. Cryst.* **38**, 426–432.
Kishimoto, S. (1997). *Nucl. Instrum. Methods Phys. Res. A*, **397**, 343–353.
Knoll, G. F. (2000). *Radiation Detection and Measurement*, 3rd ed. New York: John Wiley and Sons.
Lee, W. K. & Mills, D. M. (1992). *Rev. Sci. Instrum.* **63**, 1225–1228.
Quintana, J. P. (1991). *J. Appl. Cryst.* **24**, 261–262.